

## Design Considerations for a Transversely Polarized Target in Hall B at Jefferson Lab

---

**C.D. Keith**<sup>a,\*</sup>

<sup>a</sup>*Thomas Jefferson National Accelerator Facility, Newport News, USA*

*E-mail:* [ckeith@jlab.org](mailto:ckeith@jlab.org)

The transverse degrees of freedom of partons inside the proton are a highlight of the future experimental program in Hall B at Jefferson Lab. This program will include measuring numerous single- and double-spin asymmetries using a transversely polarized proton target and the large acceptance detector CLAS12. However, a number of technical difficulties associated with the polarized target must be addressed before these measurements can commence. In these proceedings I examine two promising target design solutions and explain why they will not work. Finally, I offer a compromise solution that will permit transverse spin measurements using the Forward Detector package of CLAS12.

*25th International Spin Physics Symposium (SPIN 2023)  
24-29 September 2023  
Durham, NC, USA*

---

\*Speaker

## 1. Introduction

Run Group H is a suite of future experiments in Hall B at Jefferson Lab that will measure single- and double-spin asymmetries for polarized electrons impinging on transversely polarized protons to access quantities related to the transverse degrees of freedom of partons inside the proton, including the Sivers and pretzelosity functions [1], the transversity distribution  $h_1$  [2], and the Generalized Parton Distribution  $E$  [3]. The proposals for each of these experiments were very well received and labelled as ‘High Impact’ by the Jefferson Lab Program Advisory Committee (PAC), meaning they should receive scheduling priority. The measurements will require the operation of a transversely polarized proton target with the CEBAF electron beam and the large acceptance detector CLAS12 [4]. The target originally described in these proposals was a frozen spin polarized target of solid hydrogen deuteride, HDice [5], that had previously only been used in low luminosity experiments with secondary beams of real photons. They were therefore *conditionally* approved, with full approval contingent on demonstrating the successful operation of HDice with a 1 nA beam of electrons [6]. Unfortunately, subsequent measurements with HDice were performed using an 8 MeV electron test beam at Jefferson Lab and found that the target polarization would last no more than a few hours at the desired beam current. It then became necessary to explore alternative target solutions in order to perform the Run Group H experiments.

In these proceedings, I review the basic operation of frozen spin polarized targets and discuss the loss of their polarization. I provide an explanation to the performance of HDice in the test measurements, examine (and discard) a possible substitute frozen spin target of dynamically polarized solid ammonia, and finally present the conceptual design of an alternative polarized target that will satisfy the requirements for the Run Group H experiments.

## 2. Spin Relaxation in Frozen Spin Targets

A frozen spin target is a scattering target whose nuclear spins are polarized in a high magnetic field and then placed in a lower magnetic field during the actual scattering experiment (Fig. 1). This scheme frees the target from the massive, high-field polarizing magnet and uses a smaller magnet to hold the polarization, allowing scattered particles to be detected with nearly  $4\pi$  acceptance. During the experiment, the target polarization decays in an exponential manner towards a thermal equilibrium polarization governed by the sample temperature  $T$  and holding field  $B$ ,

$$P(t) = (P_0 - P_{te})e^{-t/T_1} + P_{te}. \quad (1)$$

Here  $P_0$  is the polarization at time  $t = 0$ , and  $T_1$  is the spin-lattice relaxation time of the nuclear spins. Assuming the magnetic sublevels are populated according to Boltzmann statistics, the thermal equilibrium polarization  $P_{te}$  is described by the Brillouin function for particles of spin  $I$

$$P_{te} = \frac{2I+1}{2I} \coth\left(\frac{2I+1}{2I}x\right) - \frac{1}{2I} \coth\left(\frac{1}{2I}x\right) \quad (2)$$

where  $x \equiv \mu B/kT$ , with  $\mu$  being the magnetic dipole moment of the particle and  $k$  Boltzmann’s constant. For spin-1/2 particles like protons and electrons, this reduces to  $P_{te} = \tanh(x)$ .

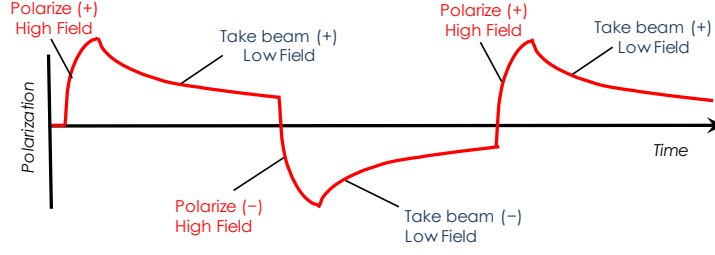


**Figure 1:** Operation of a frozen spin target in a scattering experiment.

The relaxation of nuclear spins towards thermal equilibrium is driven by the RF field produced by lattice vibrations, but only in an indirect manner. Direct coupling between the lattice and nuclear spins is very weak because the density of phonon states at typical nuclear magnetic resonance frequencies is low. In insulating solids, nuclear relaxation is instead caused by paramagnetic impurities in the material. These spins flip more frequently due to the thermal modulation of the crystal electric field which couples to the paramagnetic spins via the spin-orbit interaction. The result is an oscillating field with a nonzero component at the nuclear Larmor frequency. This leads to a nuclear spin relaxation *rate* that takes the form [7]

$$T_{1n}^{-1} \sim C \frac{\mu_e}{\mu_n} \left( \frac{\Delta B_n}{B} \right)^2 [1 - P_e^2] \tau_e^{-1}. \quad (3)$$

Here  $\mu_e$  and  $\mu_n$  are the magnetic dipole moments of the paramagnetic and nuclear spins,  $C$  is the concentration of the impurities,  $P_e$  is their thermal equilibrium polarization given by Eq. 2, and  $\Delta B_n$  is the nuclear line width.  $\tau_e$  is the correlation time of the fluctuating field, which for low concentrations we may identify with the spin-lattice relaxation time of the impurities  $T_{1e}$ . The term  $[1 - P_e^2]/T_{1e}$  can be viewed as being proportional to the probability per unit time of paramagnetic (electron) spin flips. Since  $P_e$  approaches unity at low temperature, this term goes to zero and leads to very long values of the nuclear relaxation time. Notice also, that the relaxation rate is proportional to  $C$ , the concentration of paramagnetic impurities in the sample. Taken together, these two factors explain why frozen spin targets are not generally suitable for high-intensity beams of ionizing radiation. First, the beam produces an increasing concentration of paramagnetic species in the target sample, and these provide the means for nuclear spin relaxation. Second, the beam warms the target, which decreases the polarization of the paramagnets and in turn increases the rate of nuclear polarization loss. Historically, the use of frozen spin targets has been limited to particle fluxes of order  $10^8 \text{ cm}^{-2} \text{ s}^{-1}$ .

### 3. Solid HD in Electron Beams

The HDice target is polarized in a scheme first described by Honig in 1967 [8]. A small concentration of the rotational spin isomers ortho- $\text{H}_2$  and para- $\text{D}_2$  are added to otherwise highly pure HD gas. The gas is frozen and the sample then polarized by brute force at ultralow temperatures in a very high magnetic field. Typical polarizing conditions for HDice are about 20 mK and 15 T, which yield proton and deuteron polarizations of about 0.65 and 0.15, respectively. The o- $\text{H}_2$  and

p-D<sub>2</sub> in the sample play a role similar to paramagnetic impurities: they decrease the spin-lattice times of the H and D nuclei and allow them to reach their equilibrium polarizations in a reasonable amount of time. The sample is then maintained at these extreme conditions until the o-H<sub>2</sub> and p-D<sub>2</sub> have time to convert to their nonrotational p-H<sub>2</sub> and o-D<sub>2</sub> ground states, several weeks. At this point the HD sample exhibits the extraordinarily long spin-lattice relaxation times expected for an insulating solid with no paramagnetic impurities, and it can be implemented as a frozen spin target. HD targets prepared in this manner have been utilized with beams of secondary, neutral particles [9, 10], but tests performed with electron beams have shown poor performance.

In 1975 Mano and Honig exposed polarized, spin-frozen HD at 4.2 K and 0.3 T to 10 GeV electrons at the Cornell Synchrotron [11].  $T_1$  for protons in the sample dropped from an initial value of 8 hours to 15 minutes after a dose of  $8.5 \times 10^{12} \text{ e}^- \text{ cm}^{-2}$ . Assuming a 1 cm<sup>2</sup> beam spot, this corresponds to about 23 minutes of beam at 1 nA. The authors found that melting and refreezing an irradiated sample restored its previous long value of  $T_1$  and concluded that radicals such as atomic H and D were responsible for polarization loss, not beam-induced conversion between the para- and ortho-spin isomers.

In 2012 at Jefferson Lab, tests were performed in Hall B with a 6 GeV electron beam [12]. In the most prolonged exposure, an HD sample with  $T_1 > 700 \text{ h}$  at 0.3 T lost about 98% of its initial polarization when exposed to a 1 nA beam for 14 h. This gives an average  $T_1$  of about 3 h. Beam heating was identified as the primary culprit, as thermal models indicated that the beam, slowly rastered over the face of the 1.5 cm diameter target, warmed the HD sample from its initial temperature of 0.07 K to more than 1 K.

A series of detailed measurements were again made at Jefferson Lab in 2019 using 8 MeV electrons from the Upgraded Injector Test Facility [13]. For these the magnetic holding field was increased to 1 T and efforts were made to maintain a lower sample temperature during irradiation: the length of the sample was decreased and its diameter increased, the number of aluminum cooling wires in the sample was increased, and the frequency of the beam raster was increased. NMR was used to monitor the thermal equilibrium polarization of a test sample with short  $T_1$ , and from this the sample temperature could be determined. It was found that a 0.25 nA beam warmed the sample from 0.07 K to about 0.15 K. Despite these modifications, the target lost  $1/e$  of its initial polarization after  $3.7 \times 10^{13} \text{ e}^- \text{ cm}^{-2}$ . This corresponds to an average  $T_1$  of about 2 hours at 1 nA cm<sup>-2</sup>. It was also observed that the rate of polarization loss increased with accumulated dose on the target, as predicted by Eq. 3. Finally, the rate of polarization loss increased by roughly an order of magnitude with beam on target, which is consistent with the observed beam heating and the temperature dependence of Eq. 3.

#### 4. Ammonia as a Frozen Spin Target

As described in the previous section, the radiolytic production of paramagnetic species in solid HD, combined with beam heating, makes it unsuitable for use in electron beams  $\gtrsim 0.1 \text{ nA/cm}^2$ . It is natural to ask if another polarized target sample might be less sensitive to this problem. Figure 2 shows the spin relaxation rate  $T_1^{-1}$  of three polarized proton materials as a function of accumulated electron dose: solid HD, butanol (C<sub>4</sub>H<sub>9</sub>OH), and ammonia (NH<sub>3</sub>). In each case, the relaxation rate

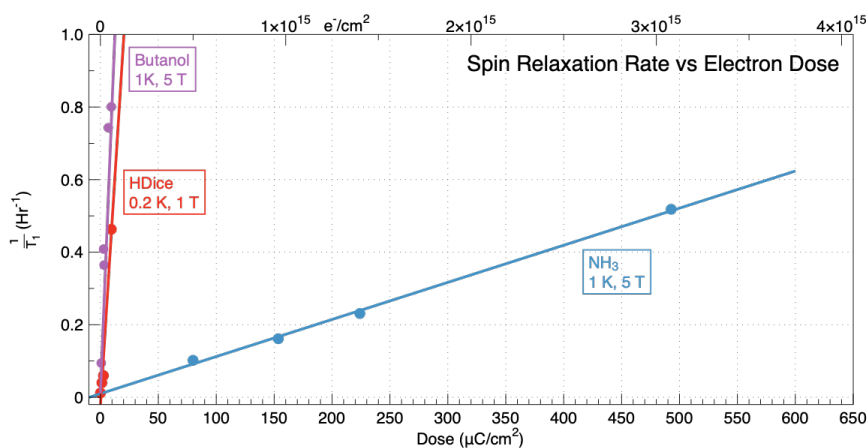


**Figure 2:** The relaxation rates for protons in butanol, solid HD, and ammonia as a function of accumulated electron dose. In all cases, the samples start as fresh, unirradiated material. The field and temperature conditions are indicated. References: HDice [13], Butanol and NH<sub>3</sub> [14]

increases linearly with dose, although the slope for ammonia is only about 1/50<sup>th</sup> of the other two. In this section, I examine ammonia as a possible frozen spin target for nA electron beams.

Dynamically polarized ammonia is the most commonly utilized polarized target material at Jefferson Lab. Proton polarizations in excess of 90% can be achieved at 1 K and 5 T, and the fraction of polarizable, free protons in the ammonia molecule (18%) is high in comparison to most other dynamically polarizable materials. Ammonia also displays a higher degree of radiation resistance than most other materials, meaning it loses polarization more slowly when exposed to ionizing radiation [15].

To realize dynamic nuclear polarization (DNP), the target sample must be intentionally doped with paramagnetic radicals at a concentration  $C \sim 10^{-4}$ . In solid ammonia the radicals are typically produced using a low-energy electron beam prior to the experiment, and the samples are stored under liquid nitrogen until needed. The radical electrons can be highly polarized under temperature and field conditions far more moderate than nuclear spins. For example, under the 1 K and 5 T conditions listed above, the electron polarization exceeds 99%. This is then transferred to nuclei via simultaneous electron-nuclear spin flip transitions driven by microwaves near the electron spin resonance frequency. The nuclear polarization can be chosen to be positive or negative, depending on whether the microwave frequency is below or above the ESR frequency. During the scattering experiment, the beam produces additional radicals in the target sample, the spin lattice relaxation rate increases above the rate of polarization transfer, and the nuclear polarization decreases. However, much of this “radiation damage” can be repaired by simply annealing the target to about 100 K for several minutes.

Once polarized, the target can be used in frozen spin mode with a lower magnetic field, or it can be continuously polarized by microwaves throughout the experiment for use with more intense beams. At Jefferson Lab, continuously polarized ammonia targets have been used with fluxes as high as  $2 \times 10^{11} \text{ s}^{-1} \text{ cm}^{-2}$ . Both frozen spin [16] and continuously polarized [17] targets have been used in Hall B during JLab’s 6 GeV era, and a new continuously polarized target with a longitudinal

orientation of the spins inside CLAS12 is described in these proceedings [18].

Dynamically polarized ammonia is clearly an attractive alternative to the brute-force polarized solid HD target originally proposed for Run Group H. In the remainder of this section, I examine the feasibility of using it in the frozen spin state with a 1 nA beam of electrons and find there is no compelling reason to pursue this operational mode over a continuously polarized version.

We start by estimating the temperature of solid ammonia when exposed to a 1 nA electron beam. The ammonia sample is taken to consist of spheres of 1 mm radius filling a 1 cm radius target cell and immersed in liquid helium. The electron beam is evenly distributed over the entire face of the target cell so that each sphere only absorbs a small fraction of the beam. Using existing data on ammonia, we then determine the field needed to achieve an initial relaxation time of  $T_1 > 200$  h, which we take as the minimum relaxation time needed for a feasible frozen spin target. The polarization will actually drop more rapidly than predicted by Eq. 1 because  $T_1$  will continuously decrease as dose accumulates on the target.

Assuming an energy deposition  $dE/dx = 2.8 \text{ MeV g}^{-1} \text{ cm}^{-2}$  for 10 GeV electrons on solid ammonia, we find that each 1 mm sphere will absorb about  $3 \mu\text{W}$  from the beam. The heat will be transported through the lattice by phonons, but these will experience a significant degree of specular reflection at the boundary between the ammonia surface and the surrounding liquid helium, limiting the heat transfer between the two. The resulting heat transfer can be described by

$$\dot{Q} = \sigma \kappa_k (T_w^4 - T_c^4). \quad (4)$$

Here  $\dot{Q}$  is the power deposited by the beam,  $\sigma$  is the surface area of the ammonia sphere,  $\kappa_k$  is the Kapitza conductance between liquid helium and solid ammonia, and  $T_c$  and  $T_w$  are the temperatures between the cold liquid bath and warm solid, respectively. We take  $\kappa_k \approx 3 \text{ W m}^{-2} \text{ K}^{-4}$  based on a survey of the literature for similar insulating materials and find that the surface of the ammonia sphere will be about 0.3 K warmer than the helium bath. The temperature gradient inside the solid ammonia due to its bulk thermal resistance will be negligible in comparison [19].

$T_1$  measurements as a function of temperature are shown for ammonia at a variety of magnetic fields in Fig. 3. They indicate that the field required to meet our desired goal of  $T_1 > 200$  h must be at least 2.5 T. Such a high field calls to question the advantages of a frozen spin target over one that is *continuously* polarized by DNP at similar field and temperature conditions (2.5 T, 0.3 K). In the latter case the sample lifetime is not characterized by its spin-lattice relaxation time but instead by a particle fluence that reduces its polarization by  $1/e$ . For ammonia this is approximately  $1 \times 10^{16} \text{ cm}^{-2}$  [15] and corresponds to about 1400 h, assuming a 1 nA electron beam distributed over a 1 cm radius. In other words, we expect a continuously polarized target to last about an order of magnitude longer in the beam than its frozen spin counterpart. DNP at 1 K and 5 T yields similarly high polarization but is operationally much easier and more time efficient.

## 5. Transverse Magnets in CLAS12

CLAS12 is comprised of two major detector packages, Central and Forward, each featuring a large, superconducting magnet to aid in tracking and identification of particles [20]. A six-coil, 2 T torus magnet is used for the Forward detector and a 5 T solenoid for the Central detector. The

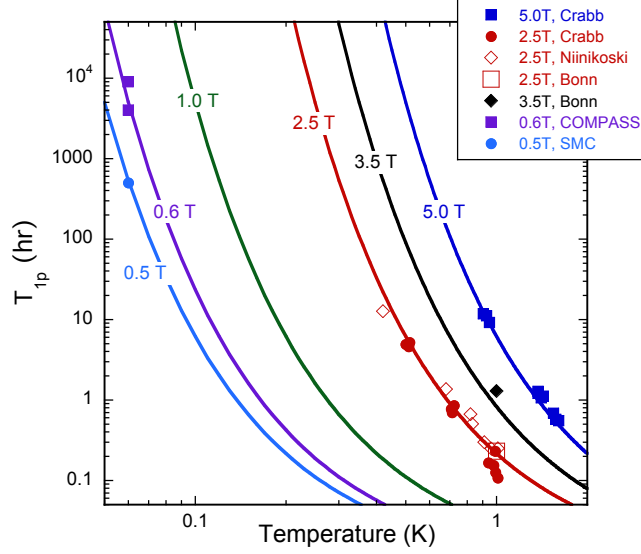


**Figure 3:** Spin-lattice relaxation times for protons in irradiated ammonia. The blue curve is a fit to the 5 T data of Crabb *et al.* according to Eq. 3. The other curves correspond to the same fit evaluated at the indicated magnetic fields. References: Crabb [21], Bonn [22], Niinikoski [23], COMPASS [24], SMC [25]. The data of Niinikoski have been scaled to reflect the low number of paramagnetic radicals in the sample. In other cases, the samples have sufficient radicals for optimal DNP.

solenoid is designed to serve three purposes. First, it bends low-energy (0.3–1.5 GeV) charged particles for spectroscopic analysis by the Central detector. Second, it focuses the copious number of Møller-scattered electrons away from the Forward detector, allowing higher data rates for the detector elements. Third, the solenoid provides the magnetic field required to dynamically polarize proton and deuteron targets in the longitudinally polarized target [18]. However, this large, longitudinally-directed field complicates the polarization of particles in the transverse direction.

The original Run Group H proposals envisioned using smaller coils around the HDice target sample to produce a net magnetic field oriented in the transverse direction. First, a combination of solenoid and Helmholtz coils would cancel the field of the CLAS12 solenoid, operating at 3 T. Second, saddle coils would generate a 0.5–1 T field in the vertical direction. To my knowledge, a detailed engineering study of these coils was never completed. Instead, the collaboration initiated an R&D project to study the use of bulk, superconducting cylindrical shells to simultaneously shield the solenoid’s longitudinal field on the outside and maintain a transverse field in its interior [26]. Initial results have been promising, but the degree to which a highly uniform transverse field can be stably trapped and maintained in the interior of the shell is unknown. For optimal dynamic polarization, this uniformity should be of order 100 ppm over the volume of the target. While this remains a highly intriguing solution to the problem, considerable work remains to demonstrate its feasibility.

Instead, the solution currently being pursued at Jefferson Lab is to simply remove the solenoid and utilize a 1 K, 5 T dynamically polarized target similar to systems used with success at JLab and elsewhere [17, 27–29]. In these systems, proton polarizations in excess of 90% and deuteron



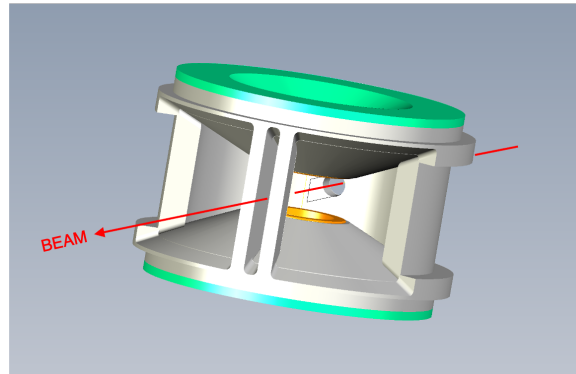


**Figure 4:** Preliminary model for a 5 T split coil polarizing magnet. The magnet features a forward aperture for scattered particles that extends  $\pm 25^\circ$  in the vertical plane and  $\pm 60^\circ$  in the horizontal.

polarizations up to 50% have been demonstrated in irradiation-doped samples of  $\text{NH}_3$  and  $\text{ND}_3$ , respectively. A model for the polarizing magnet is shown in Fig. 4. It features an aperture that extends  $\pm 25^\circ$  in the vertical plane and  $\pm 60^\circ$  in the horizontal, which is sufficient for the simultaneous  $e\gamma$  detection needed for the DVCS measurements. Thin support posts are needed in the forward direction to offset the attractive force between the upper and lower coils ( $\sim 50$  tons). In the model shown, each support spans  $\pm 5^\circ$  to  $\pm 10^\circ$ . Studies are currently underway to optimize the magnet design for both structural integrity and detection of scattered particles.

An initial design study indicates that a target cryostat can be constructed and made compatible with the existing CLAS12 forward detector, including the High Threshold Cherenkov Counter (HTCC). The HTCC is the primary system for separating scattered electrons from charged pions, kaons, and electrons, and provides full, uninterrupted azimuthal coverage and polar coverage from  $5^\circ$  to  $35^\circ$ . A new detector for DVCS protons will be designed and constructed to replace the central detector.

The largest source of background produced by the high-energy electron beam hitting the target will come from Møller scattering, and the vertical field of the polarizing magnet will concentrate the scattered electrons into an intense “sheet of flame”. These will be reduced to acceptable levels by improved shielding near the target and operating at a luminosity of  $5 \times 10^{33} \text{ cm}^{-2} \text{ s}^{-1}$ , which corresponds to approximately 2 nA on a 1 cm long  $\text{NH}_3$  target. This is lower than the maximum value currently allowed by the CLAS12 detector system ( $10^{35}$ ) but matches the number assumed in the original DVCS proposal with the HDice target.

## 6. Summary

In this article I have discussed the operation of frozen spin polarized targets and their feasibility for use with intense beams of charged particles. An insulating solid with nuclear-spin polarization loses its polarization due to the presence of paramagnetic impurities within the sample. These impurities are produced in ever-increasing numbers by the charged particle beam. The beam also heats the target material and causes it to lose polarization faster. This mechanism explains the performance of polarized solid HD samples in tests with electron beams. Similar behavior will occur in a frozen spin target of dynamically polarized ammonia.



Frozen spin targets are therefore not a viable option for the approved Run Group H series of transversely polarized target experiments in Hall B at Jefferson. Instead, the experiments will be performed using  $\text{NH}_3$  samples that are *continuously* polarized by microwave irradiation at 5 T and 1 K. A 2 nA beam impinging on a 1 cm long, 1.5 cm diameter target will provide the originally proposed luminosity of  $5 \times 10^{33} \text{ cm}^{-2} \text{ s}^{-1}$ . Under these conditions, a target sample can be used for up to a week before it needs to be annealed to repair the radiation damage produced by the beam.

## Acknowledgements

This material is based upon work supported by the U.S. Department of Energy, Office of Science, Office of Nuclear Physics under contract DE-AC05-06OR23177.

## References

- [1] H. Avakain *et al.*, “Transverse spin effects in SIDIS at 11 GeV with a transversely polarized target using the CLAS12 Detector”, [https://www.jlab.org/exp\\_prog/proposals/12/C12-11-111.pdf](https://www.jlab.org/exp_prog/proposals/12/C12-11-111.pdf).
- [2] H. Avakain *et al.*, “Measurement of transversity with dihadron production in SIDIS with transversely polarized target”, [https://www.jlab.org/exp\\_prog/proposals/12/PR12-12-009.pdf](https://www.jlab.org/exp_prog/proposals/12/PR12-12-009.pdf).
- [3] H. Avakian *et al.*, “Deeply Virtual Compton Scattering at 11 GeV with transversely polarized target using the CLAS12 Detector”, [https://www.jlab.org/exp\\_prog/proposals/12/PR12-12-010.pdf](https://www.jlab.org/exp_prog/proposals/12/PR12-12-010.pdf).
- [4] V.D. Burkert, *et al.*, Nucl. Instrum. Methods Phys. Res. A **959**, (2020) 163419.
- [5] M.M. Lowry *et al.*, Nucl. Instrum. Methods Phys. Res. A **815**, (2016) 31.
- [6] PAC39 Report, [https://www.jlab.org/exp\\_prog/PACpage/PAC39/PAC39%20Final\\_Report.pdf](https://www.jlab.org/exp_prog/PACpage/PAC39/PAC39%20Final_Report.pdf)
- [7] A. Abragam and M. Goldman, Rep. Prog. Phys. **41**, 396 (1978).
- [8] A. Honig, Phys. Rev. Lett. **19** (1967) 1009.
- [9] S. Hoblit *et al.*, Phys. Rev. Lett. **102**, 172002 (2009).
- [10] D. Ho *et al.*, Phys. Rev. Lett. **118**, 242002 (2017).
- [11] H. Mano and A. Honig, Nucl. Instrum. Methods Phys. Res. **124** (1975) 1.
- [12] M.M. Lowry, *et al.*, Proceedings of the XVth International Workshop on Polarized Sources, Targets, and Polarimetry, PoS(PSTP 2013)015.
- [13] Kevin Wei, “The Response of Polarized Protons in Solid Hydrogen-Deuteride (HD) to Electron Beams,” Ph.D. Thesis, University of Connecticut (2021).
- [14] Mikell Seely, “Dynamic Nuclear Polarization of Irradiated Target Materials”, Ph.D. Thesis, Yale University (1982).

- [15] D.G. Crabb and W. Meyer, *Annu. Rev. Nucl. Part. Sci.* **47**, (1997) 67.
- [16] C.D. Keith *et al.*, *Nucl. Instrum. Methods Phys. Res. A* **684**, (2012) 27.
- [17] C.D. Keith *et al.*, *Nucl. Instrum. Methods Phys. Res. A* **501**, (2003) 327.
- [18] P. Pandey, “Operation of a CLAS12 Longitudinally Polarized Solid Nuclear Target in RGC”, these proceedings.
- [19] T. Romanova, P. Stachowiak, and A. Jezowski, *Phys. Status Solidi B* **250**, (2013) 1870.
- [20] R. Fair *et al.*, *Nucl. Instrum. Methods Phys. Res. A* **962** (2020) 163578.
- [21] D. G. Crabb *et al.*, in *Proc. 9th Int. Symp. on High Energy Spin Physics* (1990) 289.
- [22] K. H. Althoff *et al.*, in *Proc. 9th Int. Symp. on High Energy Spin Physics* (1990) 301.
- [23] T. O. Niinikoski and J.-M. Rieubland, *Physics Letters A* **72**, (1979) 141.
- [24] A. Berlin *et al.*, in *Proc. 14th Int. Workshop on Polarized Sources, Targets, and Polarimetry* (2011) 131.
- [25] D. Adams *et al.*, *Nucl. Instrum. Methods Phys. Res. A* **437**, (1999) 23.
- [26] M. Statera *et al.*, *Nucl. Instrum. Methods Phys. Res. A* **882**, (2018) 17.
- [27] T.D. Averett *et al.*, *Nucl. Instrum. Methods Phys. Res. A* **447**, (1999) 440.
- [28] J. Pierce *et al.*, *Nucl. Instrum. Methods Phys. Res. A* **738**, (2014) 54.
- [29] J.D. Maxwell *et al.*, *Nucl. Instrum. Methods Phys. Res. A* **885**, (2018) 145.